Biomacromolecules

Article

Cite This: Biomacromolecules 2019, 20, 3200−3210

pubs.acs.org/Biomac

SET-LRP from Programmed Difunctional Initiators Encoded with Double Single-Cleavage and Double Dual-Cleavage Groups

Adrian Moreno,[†] Juan C. Ronda,[†] Virginia Cádiz,[†] Marina Galià,[†] Gerard Lligadas,*[,†,‡] and Virgil Percec*[,‡]

[†]Laboratory of Sustainable Polymers, Department of Analytical Chemistry and Organic Chemistry, University Rovira i Virgili, Tarragona 43007, Spain

[‡]Roy & Diana Vagelos Laboratories, Department of Chemistry, University of Pennsylvania, Philadelphia, Pennsylvania 19104-6323, United States

Supporting Information

ABSTRACT: The use of stimuli-cleavable difunctional initiators containing a discrete single-type cleavable junction represents a general strategy to prepare mid-chain-degradable vinylic polymers. Here, we present a series of α-haloester-type programmed initiators encoding multiple single-type and dual-type cleavable junctions. Multiple single-cleavage groups increase the cleavage rate, whereas double-dual sites provide access to multiple mechanisms for cleavage. Single-electron transfer living radical polymerization was employed to generate well-defined mid-chain-cleavable poly(methyl acrylate)s designed with low-pH, low-pH/reduction, or low-pH/UV light cleavable linkages. Kinetic studies demonstrated that the polymerizations are living when using various catalytic Cu(0) sources (wire and powder), ligands (Me_6-TREN and TREN), and solvent sources (homogeneous and "programmed" biphasic). Moreover, structural analyses by NMR and matrix-assisted laser desorption/ionization-time-of-flight confirmed the near-perfect chain-end functionality of these stimuli-cleavable polymers derived from programmed initiators. A rigorous gel permeation chromatography study demonstrated that the combination of multiple acetal, disulfide, or 2-nitroresorcinol-derived acetal junctions offer attractive possibilities in terms of selective cleavage and orthogonal degradation.

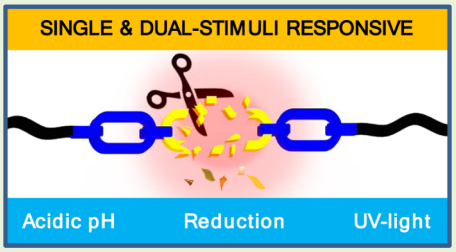

INTRODUCTION

The conception of functional polymers that can predictably respond to environmental changes through chemical or physical transitions is a field of growing importance in polymer science.[1−4] Particularly, the integration of stimuli-responsive degradable groups within the polymer main-chain or side-chain is a promising platform in the design of smart polymers for applications at the cross-frontier of chemistry and biology.[5−7] Broad interest in these materials arises due to their ability to specifically sense and respond to biologically relevant signals such as pH,[8] redox potential,[9] endogenous gases,[10] or certain enzymes.[11] Benefiting from the advent of living radical polymerization techniques, the use of stimuli-cleavable difunctional initiators facilitates the rather simple synthesis of vinyl (co)polymers with a well-defined architecture and cleavage pattern (Figure 1a).[12]

This class of telechelic polymers can convert specific stimulation to functional outputs based on the cleavage of the polymer chain into two shorter fragments while generating certain functional end-groups at the α-polymer terminus. Due to these features, a number of initiators integrating only one single-type of cleavage linkage, most of them intended for metal-catalyzed techniques,[12−17] have been proposed (Figure 1b). Noteworthy examples are disulfide-containing initiators,[18−26] which cleave upon exposure to a highly reducible environment and therefore can serve to prepare redox-responsive nanoplatforms for cellular delivery applications by means of glutathione.[27,28] Interestingly, von Delius and co-workers demonstrated that disulfide-centered polyacrylates can also split into two equally sized fragments when exposed to ultrasound activation or dynamic covalent disulfide exchange.[29] Other difunctional initiators containing cleavage entities such as hemiacetal esters (cleavable by harsh acid conditions or temperature),[30,31] Diels−Alder adduct (temperature),[32] 2-nitrobenzyl esters[33,34] and ethers[35] (UV light), 2-(pyridine-2-yl)ethyl carboxylate esters (temperature),[36] and olefin (ozone)[37,38] have been reported. As can be seen from Figure 1b, most of these initiators contain a single-type labile linkage. However, the presence of multiple identical or different degradable functionalities that are active via an identical or different mechanism and therefore provide access to either an accelerated cleavage via a single mechanism or by a combination of several mechanisms in the initiator residue could be employed to program the degradation efficiency by increasing the rate or the number of mechanisms. Indeed, the incorporation of distinct stimuli-responsive linkages would be even more interesting in terms of finer modulations. Driven by the complex functions of living organisms, dual- and

Received: June 26, 2019
Revised: July 11, 2019
Published: July 12, 2019

DOI: 10.1021/acs.biomac.9b00892
Biomacromolecules 2019, 20, 3200−3210

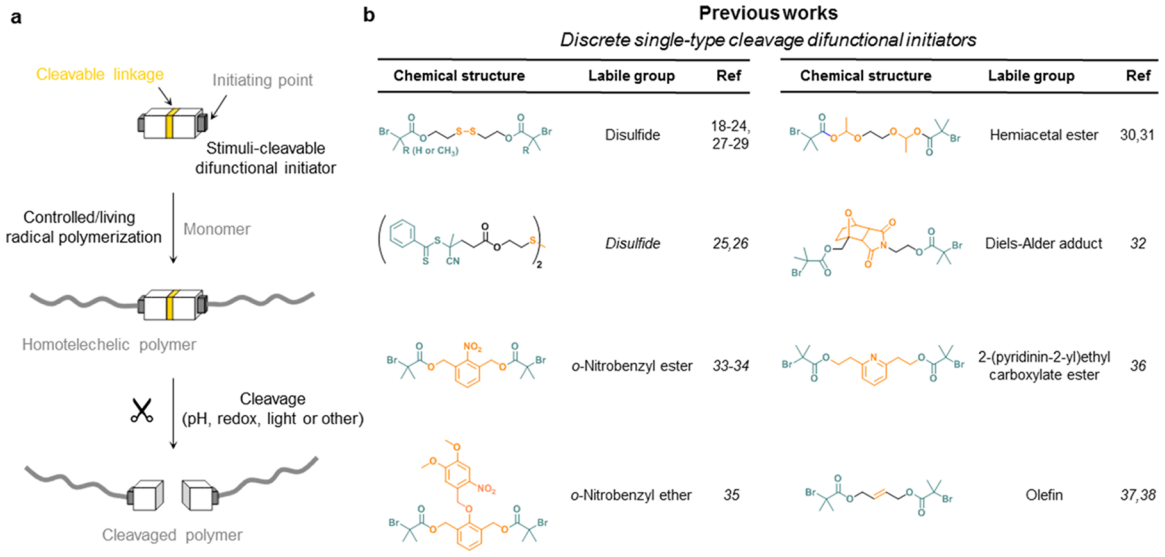

Figure 1. Living radical polymerization initiated from stimuli-cleavable difunctional initiators: (a) general synthetic approach for the preparation of mid-chain-cleavable polymers using cleavable difunctional initiators and (b) typical cleavable difunctional initiators containing a single-type cleavage linkage.

multiresponsive systems are in fact more desirable for medical and other applications compared with conventional ones containing single-type labile units since they can be used to generate programmed stimuli-responsive initiators and polymers.

In the present work, we rationally designed and synthesized three original cleavage α-haloester-type difunctional initiators sensitive to low pH (**1**), low pH/reduction (**2**), and low pH/UV light irradiation (**3**) (Figure 2). Specifically, we introduced two acid-sensitive acetal linkages in all of the initiators using the acid-catalyzed addition of alcohols to vinyl ethers as a key reaction step.[39] However, initiators **2** and **3** turned out to be also sensitive to reduction and UV light, integrating two disulfide and 2-nitroresorcinol moieties as a second type of stimuli-cleavage entities, respectively. After synthesis, these initiators were tested in the polymerization of methyl acrylate (MA) via Cu(0)-mediated single-electron transfer living radical polymerization (SET-LRP). Kinetic studies using NMR spectroscopy and gel permeation chromatography (GPC) were carried out to reveal a good control of polymerizations under various SET-LRP reaction conditions. Moreover, structural NMR and matrix-assisted laser desorption/ionization-time-of-flight (MALDI-TOF) analyses confirmed the near-perfect chain-end functionality of the synthesized polymers. Importantly, the well-defined architecture and stimuli-cleavage pattern of the resulting polymers allowed mid-chain cleavage under various mild reaction conditions (e.g., acid, reduction, and UV-light irradiation). More interesting is that mixtures of these polymers could be selectively and sequentially cleaved into two shorter fragments by the appropriate selection of stimulation even in the presence of polymers prepared from conventional stable initiators.

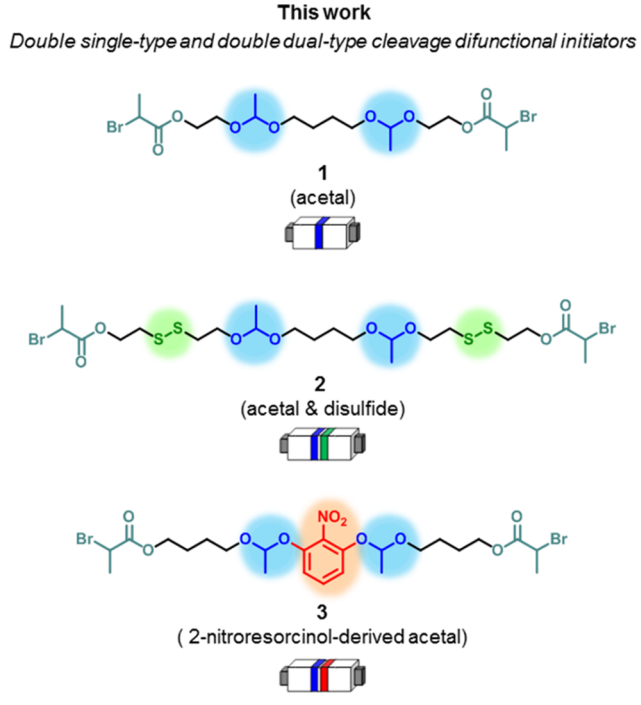

Figure 2. Chemical structure and symbol code for the double single-type (**1**) and double dual-type (**2**–**3**) cleavage difunctional initiators reported in this work. Color code in panel (c): acetal linkages, blue; disulfide linkages, green; and 2-nitroresorcinol-derived entity, red.

EXPERIMENTAL SECTION

Materials. The following chemicals were purchased from Sigma Aldrich and used as received: 2-bromopropionyl bromide (97%), anhydrous ethylene glycol (99%), 1,4-butanediol divinyl ether (98%), 1,4-butanediol vinyl ether (98%), 2-nitroresorcinol (98%), pyridinium *p*-toluensulfonate (PPTS, 99%), tris[2-(dimethylamino)ethyl]amine (Me_6-TREN, 97%), tris(2-aminoethyl)amine (TREN, 96%), copper(II) bromide (Cu(II)Br_2, 99%), dialysis tubing benzoylated (MWCO 2000), dimethylsulfoxide (DMSO, 99.7%), hydrazine hydrate (60% hydrazine), thiophenol (>99%), trans-2-[3-(4-*tert*-butylphenyl)-2-methyl-2-propenylidene]malonitrile (>98%), and potassium trifluoroacetate (KTFA, 98%). Tributylphosphine (PBu_3, 97%) and trifluoroacetic acid (TFA, 99%) were obtained from Fluka and Alfa Aesar, respectively. Methyl acrylate (MA, >99%), purchased from Sigma Aldrich, was de-inhibited by passing it through a small basic alumina pipette. 2,2,2-Trifluoroethanol (TFE, 99%) and high-performance liquid chromatography (HPLC)-grade acetonitrile

DOI: 10.1021/acs.biomac.9b00892
Biomacromolecules 2019, 20, 3200−3210

(MeCN) were obtained from Merck. HPLC-grade tetrahydrofuran (THF), acetone (synthesis grade), and ethanol (EtOH, 96%) were purchased from Scharlab. Deuterated chloroform ($CDCl_3$) was purchased from Eurisotop. Triethylamine (TEA, >99%, Merck) and dichloromethane (DCM, reagent grade) were dried over CaH_2 and distilled. Copper(0) wire (99.9% pure) of 20 gauge diameter, received from Creating Unkamen, was activated using hydrazine following a procedure developed in our lab,[40] whereas copper(0) powder (45 μm, 99.9% pure, from Sigma Aldrich) was used as received.

Methods. ^{1}H and ^{13}C NMR spectra analyses were performed on a Varian VNMR-S400 NMR instrument at 400 MHz (for ^{1}H) and 100.6 MHz (for ^{13}C). All of the chemical shifts are quoted on the δ scale in ppm based on trimethylsilane as the internal standard. For the chain-end analysis of polymers, the delay time was fixed at 10 s (d_1 = 10) and the number of scans at 100 (nt = 100). Molecular weight analysis was performed via gel permeation chromatography (GPC) using an Agilent 1200 series system equipped with three columns (PLgel 3 μm MIXED-E, PLgel 5 μm, and PLgel 20 μm from Polymer Laboratories) and an Agilent 1100 series refractive-index factor detector. THF was used as an eluent at a flow rate of 1.0 mL min^{-1}. The weight-average and number-average molecular weights of the synthesized polymers (M_w and M_n, respectively) were determined using a library of poly(methyl methacrylate) (PMMA) standards from American PSS Polymer Standards Service GmbH. Electrospray ionization (ESI) mass spectroscopy analysis was performed on an Agilent G3250AA liquid chromatography system coupled to a 6210 time-of-flight (TOF) mass spectrometer from Agilent Technologies with an ESI interface. Nominal and m/z mass are reported in daltons. Matrix-assisted laser-desorption TOF (MALDI-TOF) analysis was performed on a Voyager-DE (Applied Biosystems) instrument with a 337 nm nitrogen laser (3 ns pulse). The accelerating potential was 25 kV and the laser power 1900 units for all of the polymers. The analysis was performed using trans-2-[3-(4-*tert*-butylphenyl)-2-methyl-2-propenylidene]malonitrile as a matrix and KTFA as the cationization agent. Samples were prepared as follows: THF solution of the matrix (30 mg mL^{-1}), KTFA (10 mg mL^{-1}), and the polymer (10 mg mL^{-1}) were prepared, and the final solutions for MALDI-TOF analysis were obtained by mixing the matrix/salt and polymer solutions in a 9/1/1 volumetric ratio. After that, 1 μL of the solution mixture was deposited onto five wells of a sample plate and dried in air at room temperature before being subjected to the analysis.

Synthesis of Stimuli-Cleavage Initiator ***1***. Step I: Anhydrous ethylene glycol (30 mL, 537.94 mmol) was added to a 100 mL Schlenk round-bottom flask previously flame-dried under vacuum and purged three times with argon. The flask was equipped with a magnetic stir bar and a rubber septum. The flask was then cooled to 0 °C, and 2-bromopropionyl bromide (21.22 mmol, 2.25 mL) was added dropwise during 15 min. The resulting reaction mixture was stirred at 0 °C for an additional 3 h. After that, the crude reaction was quenched by the addition of 100 mL of water and extracted with dichloromethane (3 × 100 mL). The combined organic extracts were dried over $MgSO_4$, filtered, and evaporated under vacuum. The subsequently obtained liquid was purified by vacuum distillation (85 °C, 0.003 mbar) to yield 2-hydroxyethyl 2-bromopropionate as a viscous colorless liquid (9.8 g, 87%). ^{1}H NMR (400 MHz, $CDCl_3$, δ): 4.17−4.25 (m, 1H), 4.15 (t, 2H), 3.95 (t, 2H), 1.95 (d, 3H). ^{13}C NMR (100.6 MHz, $CDCl_3$, δ): 170.53, 67.18, 60.35, 39.93, 21.50. Step II: 2-Hydroxyethyl 2-bromopropionate (2 g, 10.15 mmol) and 1.5 mL of anhydrous dichloromethane were added to a 25 mL Schlenk tube previously flame-dried under vacuum and purged with argon. After that, PPTS (63 mg, 1% mmol) was added under argon flow. The flask was placed into a thermostatic bath at 25 °C prior to the dropwise addition of 1,4-butanediol divinyl ether (5 mmol, 0.82 mL) under an argon atmosphere. The reaction mixture was stirred for an additional 30 min, then quenched by the addition of a diluted solution of sodium carbonate ($NaHCO_3$, 5%), and subsequently extracted with DCM (3 × 20 mL). The combined organic extracts were dried using $MgSO_4$, filtered, and concentrated. The obtained crude product was purified by column chromatography (8:2 hexane/ethyl acetate, 1% TEA) to afford the initiator **1** (3.4 g, 85%) as a colorless liquid. ^{1}H NMR (400 MHz, $CDCl_3$, δ): 4.75 (q, 2H), 4.41 (q, 2H), 4.31 (t, 4H), 3.78−3.70 (m, 4H), 3.61−3.41 (m, 4H), 1.84 (d, 6H), 1.65 (m, 4H), 1.32 (d, 6H). ^{13}C NMR (100.6 MHz, $CDCl_3$, δ): 170.25, 99.71, 65.26, 65.17, 62.03, 39.85, 26.67, 21.65, 19.53. High resolution mass spectrometry (HRMS) (TOF ES$^+$) m/z: [M + H]$^+$ calcd for $C_{18}H_{32}Br_2O_8^+$, 535.0464; found, 535.0467.

Synthesis of Stimuli-Cleavage Initiator ***2***. Step I: 2-((2-Hydroxyethyl)disulfaneyl)ethyl 2-bromopropanoate was synthesized following the methodology described above for 2-hydroxyethyl 2-bromopropionate. In this case, the crude product was purified by column chromatography (20:1 hexane/ethyl acetate) to obtain the pure product as a viscous yellow liquid (8.9 g, 89%). ^{1}H NMR (400 MHz, $CDCl_3$, δ): 4.45 (q, 1H), 4.35 (t, 2H), 3.91 (t, 2H), 2.86 (t, 2H), 2.64 (t, 2H), 1.94 (t, 1H), 1.86 (d, 3H). ^{13}C NMR (100.6 MHz, $CDCl_3$, δ): 171.82, 67.25, 62.83, 41.23, 40,82, 36.92, 22.83. Step II: Initiator **2** was synthesized following the same methodology described above for compound **1**. In this case, the obtained crude product was purified by column chromatography (10:1 hexane/ethyl acetate, 1% TEA) to afford the stimuli-cleavage initiator **2** (3.9 g, 82%) as a pale-yellow liquid. ^{1}H NMR (400 MHz, $CDCl_3$, δ): 4.74 (q, 2H), 4.44 (q, 2H), 4.38 (t, 4H), 3.81−3.70 (m, 4H), 3.61−3.41 (m, 4H), 2.96 (t, 4H), 2.91 (t, 4H), 1.85 (d, 6H) 1.65 (m, 4H), 1.31 (d, 6H). ^{13}C NMR (100.6 MHz, $CDCl_3$, δ): 170.04, 99.83, 65.34, 63.71, 63.06, 39.79, 39.27, 36.64, 26.69, 21.62, 19.68. HRMS (TOF ES$^+$) m/z: [M + H]$^+$ calcd for $C_{22}H_{40}Br_2O_8S_4$, 718.9973; found, 718.9976.

Synthesis of Stimuli-Cleavage Initiator ***3***. Step I: 1,4-Butanediol vinyl ether (5 g, 56.75 mmol), 100 mL of dichloromethane, and TEA (15.8 mL, 113.5 mmol) were charged into a 250 mL flask equipped with a magnetic bar and an addition funnel under argon flow. The reaction mixture was cooled down to 0 °C in an ice bath and a solution of 2-bromopropionyl bromide (68.09 mmol, 7.2 mL) in DCM (50 mL) was added dropwise while stirring over a period of 15 min. The reaction mixture was stirred overnight at room temperature and then filtered and extracted with an aqueous solution of $NaHCO_3$ (5%, 3 × 100 mL) and water (2 × 100 mL). The combined organic extracts were dried using $MgSO_4$, filtered, and concentrated. The obtained crude product was purified by column chromatography (10:1 hexane/ethyl acetate), to afford 4-(vinyloxy)butyl 2-bromopropanoate as a yellowish liquid (10 g, 87%). ^{1}H NMR (400 MHz, $CDCl_3$, δ): 6.47 (q, 1H), 4.41−4.38 (m, 3H), 4.21 (dd, 1H), 4.06 (dd, 1H), 3.91 (t, 2H), 1.82 (d, 3H), 1.77 (m, 4H). ^{13}C NMR (100.6 MHz, $CDCl_3$, δ): 171.32, 151.98, 87.23, 65.83, 64.04, 40.24, 25.98, 24.78, 20.73. Step II: 2-Nitroresorcinol (0.3 g, 1.93 mmol) and anhydrous THF (3 mL) were charged into a 25 mL Schlenk tube previously flame-dried under vacuum and purged with argon. After that, PPTS (4.8 mg, 1% mmol) was added under argon flow, and the reaction mixture was placed in a thermostatic bath at 45 °C and a solution of 4-(vinyloxy)butyl 2-bromopropanoate (0.9 g, 3.9 mmol) in THF (1 mL) was added. The reaction mixture was stirred for an additional 3 h and after that quenched by the addition of a diluted solution of sodium carbonate ($NaHCO_3$, 5%) followed by extraction with DCM (3 × 20 mL). The combined organic extracts were dried using $MgSO_4$, filtered, and concentrated. The obtained crude product was purified by column chromatography (15:1 hexane/ethyl acetate, 1% TEA) to afford the initiator **3** (0.78 g, 65%) as an orange liquid. ^{1}H NMR (400 MHz, $CDCl_3$, δ): 7.28 (t, 1H), 6.86 (d, 2H), 5.45 (q, 2H), 4.37 (q, 2H), 4.15 (t, 4H), 3.72 (m, 2H), 3.52 (m, 2H), 1.82 (d, 6H), 1.70−1.65 (m, 8H), 1.50 (d, 6H). ^{13}C NMR (100.6 MHz, $CDCl_3$, δ): 170.22, 148.76, 130.57, 110.02, 109.91, 100.77, 65.60, 64.90, 40.18, 25.92, 25.25, 21.64, 19.62. HRMS (TOF ES$^+$) m/z: [M + H]$^+$ calcd for $C_{24}H_{35}Br_2NO_{10}$, 656.0628; found, 656.0624.

General Procedure for the Cu(0)-Catalyzed SET-LRP. This procedure is representative for all of the polymerizations conducted herein. The polymerization of MA using initiator **1** in DMSO under the conditions of $[MA]_0/[\mathbf{1}]_0/[Me_6\text{-TREN}]_0$ = 222/1/0.2 is described. Difunctional initiator **1** (26.7 mg, 0.05 mmol) was dissolved in MA (1 mL, 11.10 mmol) and charged in a 25 mL Schlenk tube together with DMSO (0.5 mL) and Me_6-TREN (2.8 μL, 0.01 mmol). Then, the reaction mixture was deoxygenated by six freeze−pump (1 min)−thaw cycles. Next, 12.5 cm of a hydrazine-

DOI: 10.1021/acs.biomac.9b00892
Biomacromolecules 2019, 20, 3200−3210

Scheme 1. Synthetic Strategy for the Stimuli-Responsive Programmed Difunctional Initiators

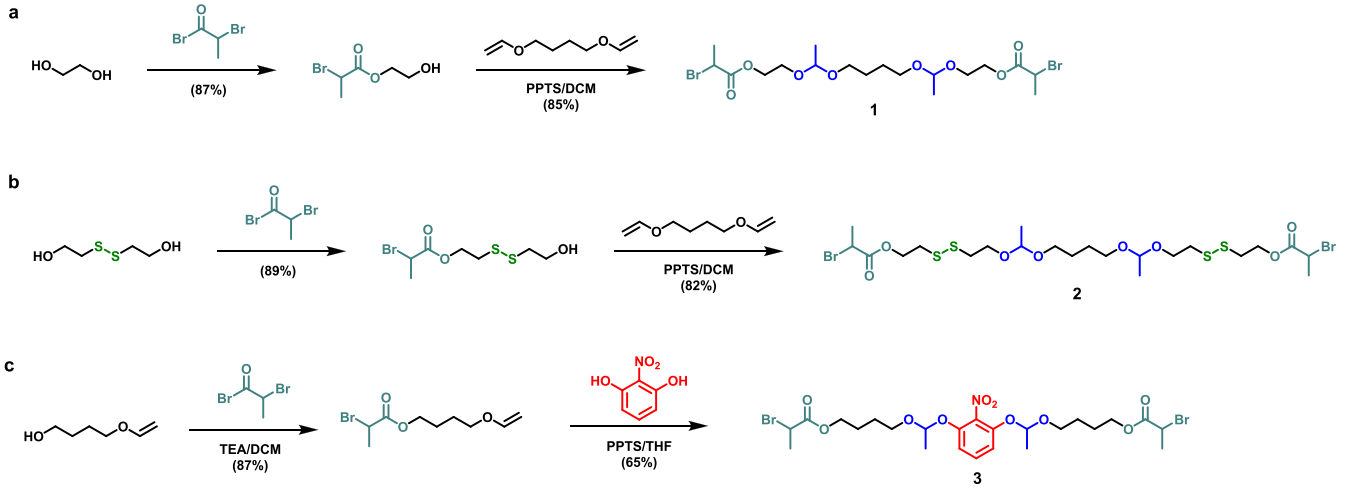

activated Cu(0) wire, wrapped around a Teflon bar, was introduced under a strong positive flow of argon and held above the reaction mixture using an external neodymium magnet. Two additional freeze−pump−thaw cycles were applied. After that, the reaction mixture was placed in a thermostatic bath at 25 °C. After approximately 1 min, the stir bar wrapped with the Cu(0) was dropped gently into the reaction mixture. The introduction of the Cu(0) wire defines $t = 0$. Only for kinetic experiments, samples were taken at determined times by purging the side arm of the Schlenk tube with argon for 1 min using a deoxygenated glass syringe and a stainless-steel needle. The collected samples were dissolved in $CDCl_3$ and quenched by exposure to air. After that, monomer conversion was determined by ^{1}H NMR spectroscopy. To determine the M_n and M_w/M_n of PMA-**1** by GPC, the solvent and monomers were eliminated under reduced pressure and the resulting residue was immediately dissolved in THF and filtered under basic alumina to remove Cu(II)Br_2 residues.

General Procedure for the Thio-Bromo "Click" Modification of Poly(methyl acrylate) (PMA) with Thiophenol.[41,42] In a 5 mL bottom vial equipped with a magnetic stirrer and a rubber septum, thiophenol (0.06 equiv) and distilled TEA (0.06 equiv) were added into a solution of the corresponding polymer (0.01 equiv) in MeCN (2 mL) under argon flow. The reaction mixture was stirred at room temperature for 3 h. Then, the resulting modified PMA was dialyzed against acetone. The obtained polymer was dried under vacuum until constant weight before ^{1}H NMR and MALDI-TOF analyses.

*Mid-Chain Acid Cleavage of PMA-**1**, **2**, and **3** and Mixtures Containing these Polymers with TFA.* A solution of polymer (50 mg) in 2 mL of THF was placed in a bottom vial equipped with a small magnetic bar. After that, TFA (80 μL, 0.1 M) was added and the resulting reaction mixture was stirred for 1 h at room temperature. The resulting solution was passed through a small basic alumina column before GPC analysis. Degradation was in some cases performed in the $CDCl_3$ solvent to allow direct ^{1}H NMR analysis.

*Mid-Chain Reductive Cleavage of PMA-**2** and Mixtures Containing this Polymer with PBu_3.* A solution of PMA-**2** (50 mg) in 5 mL of anhydrous THF was placed in a bottom vial equipped with a small magnetic bar. After that, PBu_3 (200 μL, 100 equiv) was added. The reaction mixture was stirred for 1 h at room temperature. The resulting solution was immediately analyzed by GPC.

*Mid-Chain Photodegradation of PMA-**3** and Mixtures Containing this Polymer with UV Light.* A solution of PMA-**3** (50 mg) in 2.5 mL of THF was placed in a bottom vial equipped with a small magnetic bar. The reaction mixture was stirred and subjected to UV light with four 9W UV lamps (λ = 365 nm) during 90 min at room temperature. The resulting solution was immediately analyzed by GPC.

RESULTS AND DISCUSSION

Synthetic Strategy for the Programmed Stimuli-Cleavage Difunctional Initiators. As illustrated in Scheme 1a,b, the synthesis of initiators **1** and **2** was performed in two

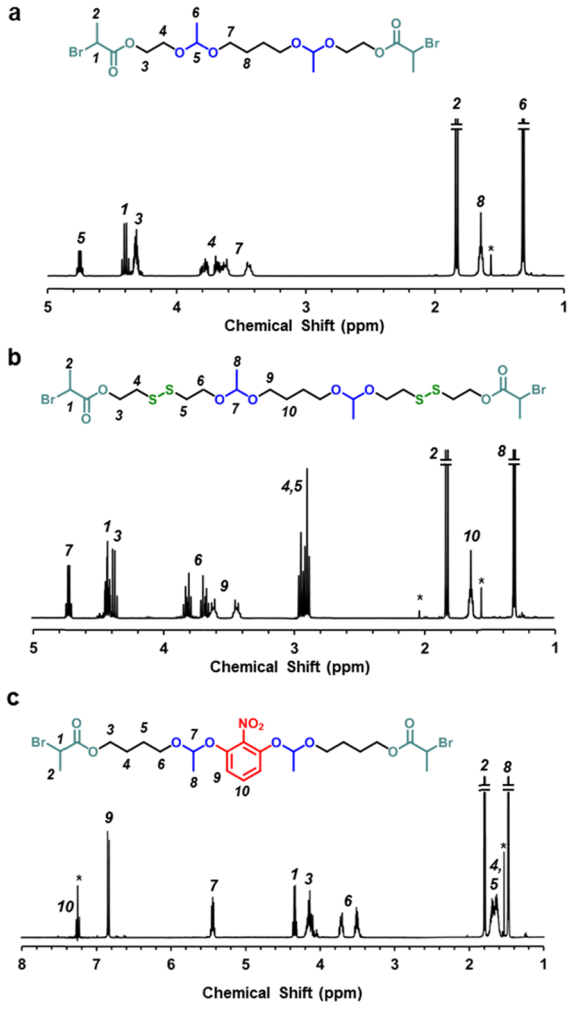

Figure 3. ^{1}H NMR spectra of the stimuli-cleavage difunctional initiators (a) **1**, (b) **2**, and (c) **3** in $CDCl_3$. ^{1}H NMR resonances from residual solvents are indicated with "*".

DOI: 10.1021/acs.biomac.9b00892
Biomacromolecules 2019, 20, 3200−3210

Scheme 2. SET-LRP Synthesis of Mid-Chain-Cleavable PMA Using the Single and Dual Stimuli-Responsive Programmed Difunctional Initiators

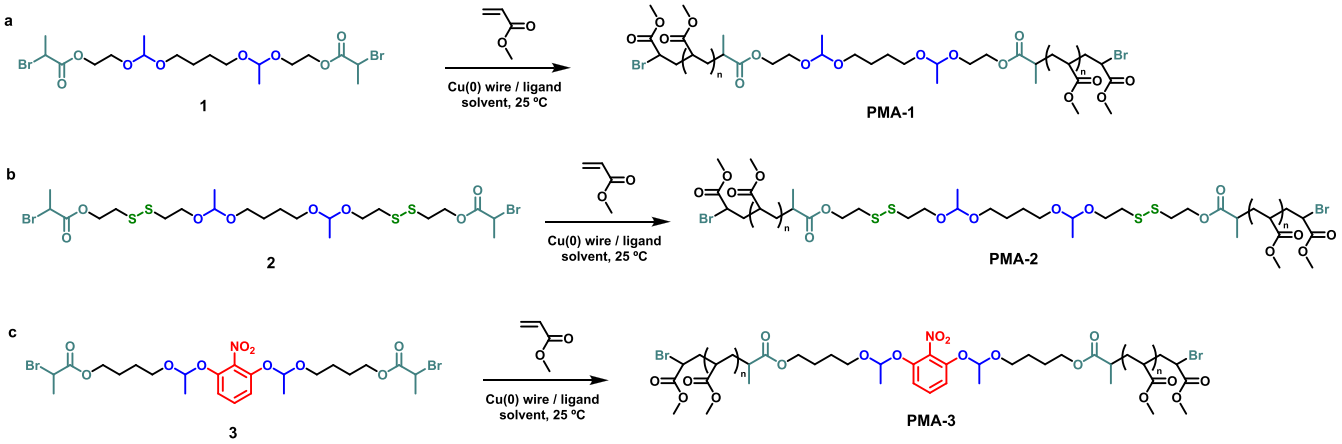

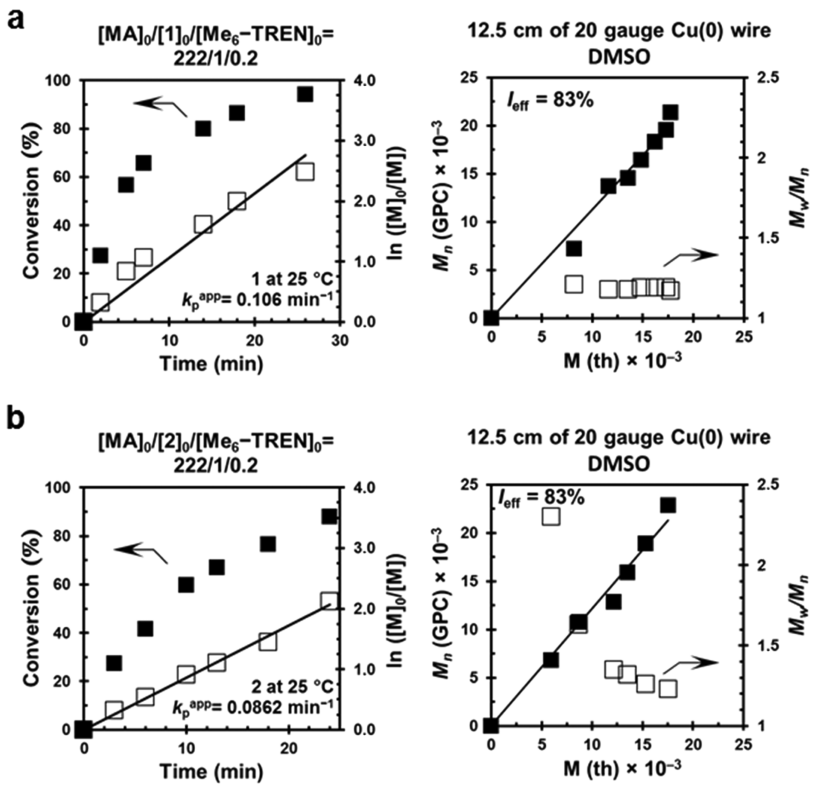

Figure 4. Monomer conversion, kinetics plots, and evolution of experimental M_n (GPC) and M_w/M_n values, based on the calibration by PMMA standards versus theoretical M(th) values for the SET-LRP of MA initiated from difunctional initiators (a) **1** and (b) **2** in DMSO at 25 °C. Reaction conditions: MA = 1 mL, DMSO = 0.5 mL, $[MA]_0/[initiator]_0/[Me_6\text{-TREN}]_0$ = 222/1/0.1 using 12.5 cm of a hydrazine-activated Cu(0) wire (20 gauge diameter).

simple steps using commercially available diols such as ethylene glycol and 2-hydroxyethyl disulfide as starting materials.

In the first step, one equivalent of 2-bromopropionyl bromide was attached to the corresponding diol through esterification of a single hydroxyl group. Importantly, the use of excess diol as well as no base, to quench the released HBr, is crucial to minimize the formation of the undesired diester. The second step was the conjugation of the obtained compound with 1,4-butanediol divinyl ether at room temperature in the presence of PPTS in DCM under rigorous anhydrous conditions. Overall, **1** and **2** were readily prepared with an overall yield of around 75%. The chemical structure of the purified initiators was confirmed by ^{1}H NMR, ^{13}C NMR, and HSQCAD NMR analyses (Figures 3a,b and S1−S4). The most characteristic ^{1}H NMR signals of both initiators are those corresponding to methyl and methyne groups of the acetal moieties at 1.3 and 4.7 ppm, respectively. Alternatively, initiator **3** (Figure 2) was synthesized from 1,4-butanediol vinyl ether, that is, by esterification with 2-bromopropionyl bromide in the presence of excess TEA followed by the reaction with 2-nitroresorcinol in the presence of PPTS (Scheme 1c). In this case, acetal linkage formation was more effective at higher temperatures (45 °C). Structural NMR

DOI: 10.1021/acs.biomac.9b00892
Biomacromolecules 2019, 20, 3200−3210

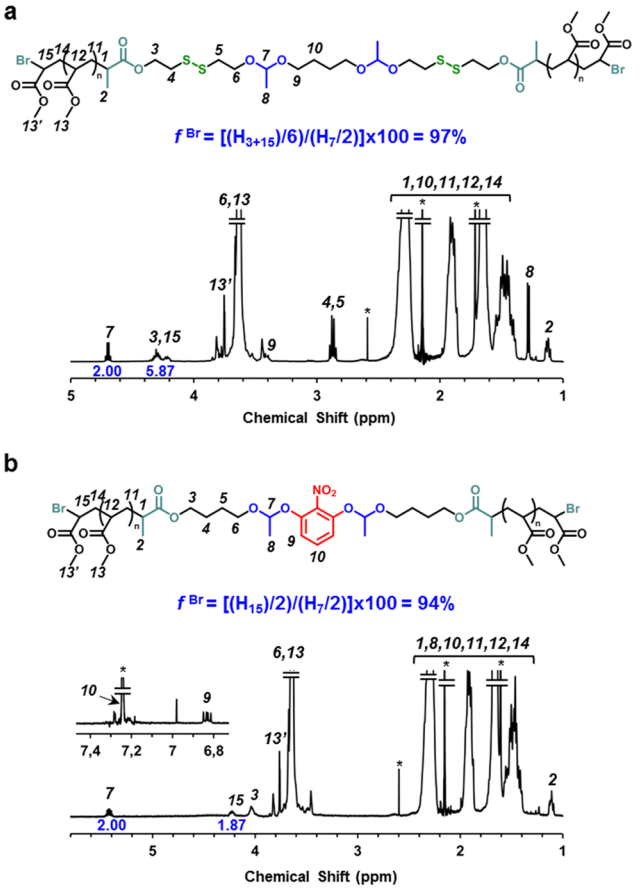

Figure 5. ^{1}H NMR spectra of mid-chain-cleavable (a) PMA-**2** and (b) PMA-**3** prepared by Cu(0) wire-catalyzed SET-LRP from difunctional initiators **2** and **3**, respectively. Reaction conditions: (a) MA = 1 mL, acetone/H_2O (8:2, v/v) = 0.5 mL, $[MA]_0/[\mathbf{2}]_0/[TREN]_0/[Cu(II)Br_2]_0$ = 222:1:0.4:0.2 using 12.5 cm of a hydrazine-activated Cu(0) wire (20 gauge diameter); and (b) MA = 1 mL, DMSO = 0.5 mL, $[MA]_0/[\mathbf{3}]_0/[Me_6\text{-TREN}]_0$ = 222:1:0.1 using 12.5 cm of a hydrazine-activated Cu(0) wire (20 gauge diameter). PMA-**2** and **3** were isolated at 89 and 94% monomer conversion after kinetic experiments. ^{1}H NMR resonances from residual solvents are indicated with ⁎.

characterization confirmed the structure of **3**, which was obtained with an overall yield of around 57% (Figures 3c and S5, S6). According to the difunctional nature of this initiator, the ^{1}H NMR integral ratio of the peaks 2/8 was determined to be 1/1. Additional structural confirmation for compounds **1**−**3** was obtained by high-resolution mass spectrometry (see Experimental Section).

Polymerization of MA by SET-LRP from the Programmed Difunctional Initiators 1−3. After synthesis, compounds **1**−**3** served as programmed difunctional initiators for the polymerization of MA using Cu(0)-mediated SET-LRP (Scheme 2). These compounds produce symmetric telechelic poly(MA)s with centrally located acetal (PMA-**1**), acetal/disulfide (PMA-**2**), and 2-nitroresorcinol-derived acetal (PMA-**3**) labile functions. First, their performance was investigated in DMSO using a Cu(0) wire catalyst and Me_6-TREN as the ligand at 25 °C. The polymerizations were conducted at a target M_n of ∼ 20 000 g mol^{-1} ($[MA]_0/[initiator]_0$ = 222) using 12.5 cm of hydrazine-activated Cu(0) wire (20 gauge diameter).

Importantly, the synthesized PMAs showed controlled M_n and low M_w/M_n values and monomodal GPC traces as expected for well-controlled polymerizations (Figure S7). Kinetic studies using NMR to determine monomer conversion and GPC to estimate experimental M_n and M_w/M_n values demonstrated the living radical polymerization features of SET-LRP. As representative examples, kinetics for the SET-LRP of MA initiated from **1** and **2** are shown in Figure 4. Both polymerizations were fast, achieving above 90% conversion in less than 30 min. It can be seen that the molar mass of the polymer increased monotonically and agreed well with the predicted values assuming 100% initiator efficiency.

Indeed, the linear increase of $\ln[M]_0/[M]$ with time supports a constant concentration of active species throughout the entire reaction. Next, to further study the performance and stability of these initiators, selected experiments were performed under a range of SET-LRP reaction conditions.[17] The solvent, Cu(0) form, and ligand were varied. First, alternative homogeneous reaction mixtures were checked. For instance, well-defined PMA-**1** and **3** were successfully prepared in a mixture of TFE/H_2O (9:1, v/v) under strictly identical reaction conditions (Figure S8a,b).[43] The use of Cu(0) powder in EtOH delivered PMA-**1** with M_n close to the theoretical value (19 500 vs 17 350 g mol^{-1}) showing a GPC curve (M_w/M_n = 1.19) with no shoulders or tails (Figure S8c). Finally, a "programmed" biphasic SET-LRP system based on an aqueous mixture of acetone, which is one of the most representative non-disproportionating solvents, was also investigated.[44−54] SET-LRP of MA was conducted in an acetone/water mixture (8:2, v/v) using Cu(0) wire. In this case, Me_6-TREN was replaced with the less expensive TREN ligand.[55] According to our previous studies, the external addition of a small amount of $Cu(II)Br_2$ deactivator to the water phase was necessary to obtain well-defined polymers from **1** and **2** (Figure S8d,e). Under these conditions, SET-LRP occurred in a biphasic reaction mixture, in which polymerization occurs in the organic phase and disproportionation of "in situ"-generated Cu(I)Br into Cu(0) and $Cu(II)Br_2$ takes place in the aqueous phase. Digital images and details on this system can be found in Figure S9.

To verify these results, the resulting polymers were characterized by ^{1}H NMR to demonstrate the telechelic nature and "livingness" of both α,ω-bromine chain-ends. As representative examples, ^{1}H NMR spectra of purified polymers PMA-**2** and **3**, prepared under different reaction conditions, are shown in Figure 5. In both cases the bromine chain-end functionality could be determined by integrating the peaks corresponding to the α-bromo chain-end $-C\underline{H}(COOCH_3)Br$ with the methine acetal protons of the initiator residue (i.e., signals 15 and 7 in Figure 5). Irrespective of the initiator and reaction conditions, NMR analysis supports a high end-group fidelity (f^{Br} > 95%). Further evidence for the well-defined structure of the synthesized polymers was provided by MALDI-TOF MS spectrometry analysis. A low-molar-mass PMA-**1** sample was prepared at $[MA]_0/[\mathbf{1}]_0$ = 50 (target M_n ∼ 4800 g mol^{-1}). This reaction also resulted in a near-quantitative conversion (97%), narrow molecular weight distribution, and well-defined molar mass, indicating a living polymerization.

As can be seen in Figure 6a, PMA-**1** showed a single distribution of peaks, separated by 86 mass units, attributable to PMA-**1**/K^+ species. As expected for a polymer with a perfect bromine chain-end functionality, this distribution completely vanished and a new series of peaks emerged 58 units above the parent distribution after thio-bromo "click chemistry" with

DOI: 10.1021/acs.biomac.9b00892
Biomacromolecules 2019, 20, 3200−3210

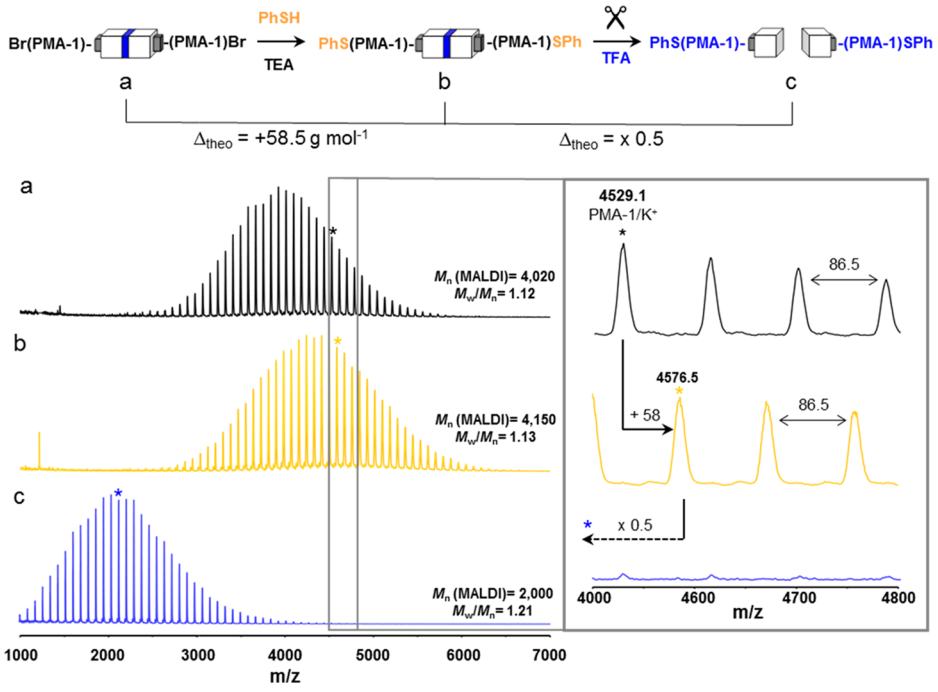

Figure 6. MALDI-TOF spectra of PMA-**1** (a) isolated at 97% monomer conversion ($[MA]_0/[\mathbf{1}]_0/[Me_6\text{-TREN}]_0$ = 50:1:0.2 in DMSO), (b) after thio-bromo click reaction at chain-ends using thiophenol, and (c) after acid-catalyzed hydrolysis of the thioetherified polymer using TFA in THF. Magnified regions confirm the expected peak-to-peak spacing for the MA repeating unit and the near-perfect bromine chain-end functionality of the synthesized polymer. Bond cleavage information: TFA treatment produces the selective acid hydrolysis of acetal linkages. The expected degradation products are shown in Figure S10a.

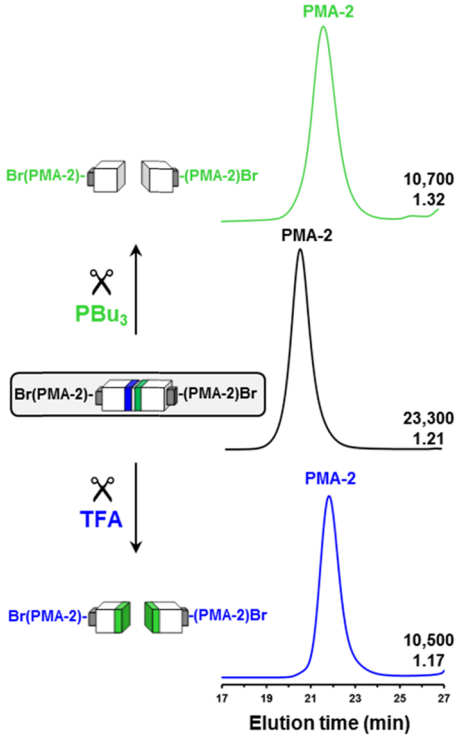

Figure 7. GPC traces for PMA-**2** before (black) and after either acid (blue) or reductive (green) treatment to promote mid-chain cleavage. Numbers shown in each panel correspond to M_n (GPC) and M_w/M_n, respectively, from the top to bottom. Bond cleavage information: PBu_3 and TFA treatments produce the selective cleavage of disulfide and acetal linkages, respectively. The expected degradation products are shown in Figure S10b.

thiophenol (Figure 6b).[41,42] An additional proof of the symmetric nature of the synthesized polymers was obtained after TFA treatment of PMA-**1** after thioetherification. Within an hour, MALDI-TOF analysis delightfully illustrated the complete vanishing of the series of peaks centered at approximately 4300 g mol^{-1}. Meanwhile, acetal mid-chain hydrolysis resulted in the appearance of only one new series of peaks with half the M_n, thus confirming the acid-catalyzed hydrolysis of the acetal linkages to the corresponding alcohols and carbonyl compound (acetaldehyde) (Figure 6c).[56] Figure S10a depicts the corresponding degradation products. This two-step chain-end modification/mid-chain cleavage process could also be monitored by ^{1}H NMR analysis (Figure S11). Overall, these observations confirm the expected polymer architecture (i.e., a homotelechelic structure with near-perfect bromine chain-ends and discrete mid-chain labile linkages) and are in agreement with previous studies from different laboratories.[57−60]

Stimuli-Responsive Mid-Chain Cleavage of PMA-1, 2, and 3 as well as Mixtures Therefrom. The ability of the synthesized polymers to sense various stimuli (i.e., acidic hydrolysis, reduction, or UV-light irradiation) and suffer mid-chain cleavage was systematically investigated by GPC. As observed in the previous section, the cleavage of PMA-**1**, designed with single-type mid-chain acetal cleavage linkages, could be carried out at room temperature in a THF/TFA solution. Under these conditions, with 50 mg of the polymer in 2 mL of THF/0.1 M TFA solution, GPC analysis also revealed the controlled reduction in the size of PMA-**1** with a higher molar mass as a result of its well-defined architecture and cleavage pattern (Figure S12). Importantly, acidic cleavage did not compromise the M_w/M_n of the resulting polymer due to the simultaneity of the divergent SET-LRP chain growth. In

DOI: 10.1021/acs.biomac.9b00892
Biomacromolecules 2019, 20, 3200−3210

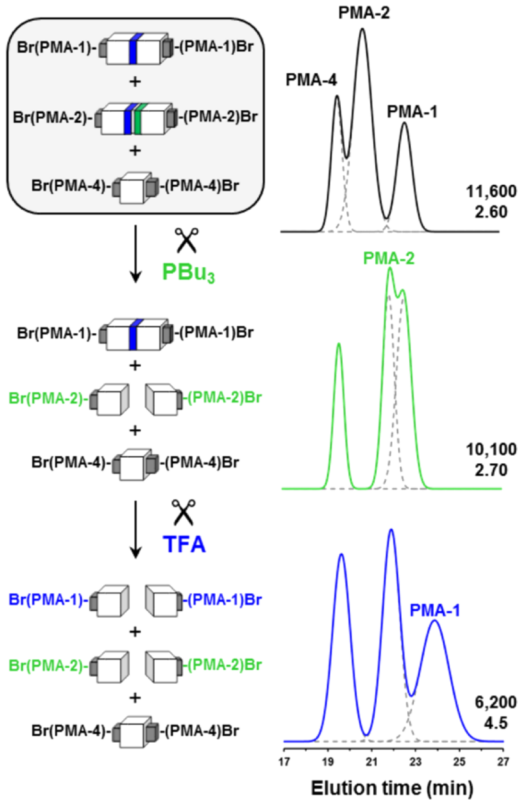

Figure 8. GPC traces for a mixture of PMA-**1** (M_n = 5300 g mol^{-1}, M_w/M_n = 1.18), PMA-**2** (M_n = 23 300 g mol^{-1}, M_w/M_n = 1.21), and PMA-**4** (M_n = 54 550 g mol^{-1}, M_w/M_n = 1.17) before (black) and after sequential reductive (green) and acid (blue) treatments to promote mid-chain cleavage. Numbers shown in each panel correspond to multipeak M_n (GPC) and M_w/M_n, respectively, from the top to bottom. The individual components from the fits to a multipeak Gaussian distribution are also shown by gray dashed lines. Bond cleavage information: PBu_3 and TFA treatments produce the selective cleavage of disulfide and acetal linkages, respectively. The expected degradation products are shown in Figure S10.

addition, it is important to highlight that the M_w/M_n experimental data are close to those expected theoretically after the mid-chain cleavage of a symmetric telechelic polymer.[61] Next, PMA-**2**, which integrates mid-chain acetal and disulfide linkages, was subjected to strictly identical acidic conditions (compare black and blue GPC traces in Figure 7).

As expected, the GPC analysis of the resulting polymer revealed the shift of the GPC trace to longer elution times compared with the parent polymer as a result of the acid-catalyzed hydrolysis of acetal moieties (Figure S10b). Taking advantage of the second stimuli-cleavage linkage in PMA-**2** (disulfide), we also proceeded to test its reductive cleavage using an excess of PBu_3. Disulfide bonds are well-known redox-sensitive linkages (Figure S10b).[62] The green GPC trace in Figure 7 confirms the reductive cleavage of the centrally located disulfide labile bonds. It is noteworthy that GPC traces after cleavage appear at approximately the same elution time irrespective of the type of treatment, that is, acid hydrolysis or reduction. These results confirm the dual responsiveness of the centrally located initiator residue resulting from the SET-LRP of MA initiated from **2**. The dual-response of the central degradable PMA-**3** core was also investigated (Figure S13). According to the literature,[63] the 2-nitroresorcinol-derived acetal linkage is a promising platform because it offers both chemodegradation (acid hydrolysis) and photodegradation over a wide range of spectrum (UV to near-infrared regime). Upon UV irradiation for 90 min, GPC analysis revealed that the M_n of PMA-**3** (M_n = 23 640 g mol^{-1}, M_w/M_n = 1.29) was reduced approximately by half as a result of the central location of the 2-nitroresorcinol group (compare black and red GPC traces in Figure S13). Otherwise, full reduction was also observed by GPC after acid treatment (blue curve). In this case, both chemo- and photodegradation treatments are expected to deliver equivalent polymers with the hydroxyl group at the α-polymer chain-end (Figure S10c).

Encouraged by these results, we investigated the cleavage behavior of representative mixtures of these polymers. For instance, selective cleavage of PMA-**2** in the presence of PMA-**1** was possible under reductive conditions. Thus, upon treating a 50 wt % mixture of PMA-**1** and PMA-**2** with excess PBu_3, only PMA-**2** beaked up, whereas the part of the mixture-based polymer chains with only acetal-type labile entities remained stable (compare black and green GPC traces in Figure S14). Next, the remaining telechelic PMA-**1** could be further split into two shorter fragments when the conditions were turned to acidic (compare green and blue GPC traces in Figure S14).

In the second experiment, a control PMA-**4**, prepared by SET-LRP of MA using the conventional bis(2-bromopropionyl)ethane (BPE) difunctional initiator with no labile core, was added to this mixture of polymers (see Figures S10 and S15 for details of PMA-**4**). Interestingly, when the reduction/acid sequential degradation protocol was applied to this tricomponent mixture of polymers, only the GPC trace of the control polymer remained stable after the second step, whereas the GPC traces of the two responsive polymers shifted to longer elution times (Figure 8). Furthermore, we could also address the selective photocleavage of PMA-**3** in the presence of PMA-**1** (Figure S16). Finally, a series of sequential degradations were performed to showcase that a mixture of PMA-**2** and PMA-**3** can undergo orthogonal degradation taking advantage of the independent degradation chemistries of disulfide and 2-nitroresorcinol acetal linkages. Delightfully, the degradation of both polymers could be successfully addressed individually and sequentially (Figure 9). Thus, reductive conditions (dashed arrow) only induced a mid-chain cleavage of PMA-**2** with no impact on 2-nitroresorcinol-derived acetal moieties, whereas UV-light irradiation (solid arrow) only impacted the photosensitive polymer PMA-**3**.

In the second step, the cleavage of the residual polymer could be performed by applying the complementary treatment. It is worth mentioning that simultaneous cleavage of both could also be conducted via acid-catalyzed acetal hydrolysis (dash−dot arrow) or alternatively by applying reductive treatment combined with UV-light irradiation (data not shown). Overall, these results demonstrate that the originality of these initiators relies not only on their individual chemical structures/responsive profiles but also on the possibilities that their combinations offer.

CONCLUSIONS

Three novel cleavable α-haloester-type programmed difunctional initiators were synthesized and used to deliver well-defined mid-chain-cleavable PMAs with single and dual response. Specifically, the initiators **1**−**3** and the corresponding polymers are sensitive to low pH, low pH/reduction, or low pH/UV-light irradiation because they integrate acetal, acetal/disulfide, or 2-nitroresorcinol-derived acetal labile linkages.

DOI: 10.1021/acs.biomac.9b00892
Biomacromolecules 2019, 20, 3200−3210

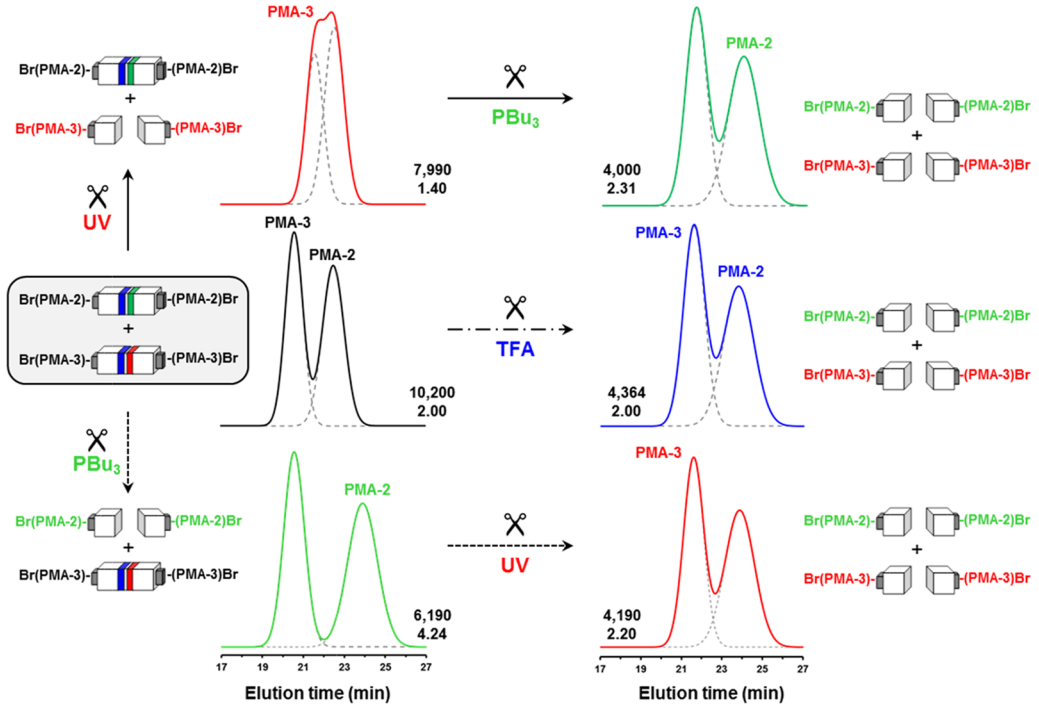

Figure 9. GPC traces for a mixture of PMA-**2** (M_n = 6200 g mol^{-1}, M_w/M_n = 1.20) and PMA-**3** (M_n = 23 640 g mol^{-1}, M_w/M_n = 1.24) demonstrating orthogonal degradation: initial mixture (black GPC trace), sequential reductive and UV-light treatments (dashed arrow), sequential UV-light and reductive treatments (solid arrow), and acid treatment (dash−dot arrow). Numbers shown in each panel correspond to multipeak M_n (GPC) and M_w/M_n, respectively, from the top to bottom. The individual component from the fits to a multipeak Gaussian distribution are also shown by gray dashed lines. Bond cleavage information: PBu_3 treatment produces the selective cleavage of disulfide linkages, whereas exposure to TFA and UV light selectively cleaves 2-nitroresorcinol-derived acetal junctions. The expected degradation products are shown in Figure S10b,c.

Polymerization studies conducted under various Cu(0)-catalyzed SET-LRP conditions resulted in a near-quantitative conversion, narrow molecular weight distribution, well-defined molar mass, and high end-group fidelity, indicating well-controlled polymerizations. Remarkably, the precise insertion of mid-chain stimuli-responsive labile units within a PMA backbone allowed its cleavage under various conditions (i.e., acid, reduction, and UV-light irradiation). It is encouraging that the cleavage of some di- and tricomponent polymer mixtures could also be addressed selectively and sequentially by the selection of the appropriate stimuli. Overall, we envision that taking advantage of the broad monomer scope of SET-LRP, mixtures of vinylic (co)polymers synthesized from difunctional initiators **1**, **2**, and **3** or other stimuli-cleavage di- and multifunctional initiators inspired from them, in combination with nonlabile initiators such as BPE or peptoid-type initiators,[64] can provide a promising framework for creating nanoscale templates for advanced biomaterial, biological, and other applications. Research on developing degradable drug delivery devices based on these initiators is currently being carried out in our laboratories and will be reported soon.

■ ASSOCIATED CONTENT

Supporting Information

The Supporting Information is available free of charge on the ACS Publications website at DOI: 10.1021/acs.biomac.9b00892.

Structural characterization of initiators **1**−**3**; SET-LRP of MA initiated with **1**−**3**; mid-chain cleavage of PMA-**1**, PMA-**2**, PMA-**3** and mixtures; ^{13}C NMR spectrum of **1** in $CDCl_3$ (Figure S1); HSQCAD spectrum of **1** in $CDCl_3$ (Figure S2) (PDF)

■ AUTHOR INFORMATION

Corresponding Authors

*E-mail: gerard.lligadas@urv.cat (G.L.).
*E-mail: percec@sas.upenn.edu (V.P.).

ORCID

Marina Galià: 0000-0002-4359-4510
Gerard Lligadas: 0000-0002-8519-1840
Virgil Percec: 0000-0001-5926-0489

Notes

The authors declare no competing financial interest.

■ ACKNOWLEDGMENTS

Financial support from the National Science Foundation Grants DMR-1066116 and DMR-1807127 and the P. Roy Vagelos Chair at the University of Pennsylvania (to V.P.) are gratefully acknowledged. We also thank Spanish Ministerio de Ciencia, Innovación y Universidades, through project MAT2017-82669-R (to G.L. and J.C.R.) and FPI grant BES-2015-072662 (to A.M.) and the Serra Hunter Programme of the Government of Catalonia (to G.L.).

■ REFERENCES

(1) Wei, M.; Gao, Y.; Li, X.; Serpe, M. J. Stimuli-Responsive Polymers and their Applications. *Polym. Chem.* **2017**, *8*, 127−143.
(2) Hu, X.; Zhang, Y.; Xie, Z.; Jing, X.; Bellotti, A.; Gu, Z. Stimuli-Responsive Polymersomes for Biomedical Applications. *Biomacromolecules* **2017**, *18*, 649−673.

DOI: 10.1021/acs.biomac.9b00892
Biomacromolecules 2019, 20, 3200−3210

(3) Shen, J.; Wang, Z.; Sun, D.; Xia, C.; Yuan, S.; Sun, P.; Xin, X. pH-Responsive Nanovesicles with Enhanced Emission Co-Assembled by Ag(I) Nanoclusters and Polyethyleneimine as a Superior Sensor for Al3+. *ACS Appl. Mater. Interfaces* **2018**, *10*, 3955−3963.
(4) Ji, J.; Li, X.; Wu, T.; Feng, F. Spiropyran in Nanoassemblies as a Photosensitizer for Photoswitchable ROS Generation in Living Cells. *Chem. Sci.* **2018**, *9*, 5816−5821.
(5) Bawa, K. K.; Oh, J. K. Stimulus-Responsive Degradable Polylactide-Based Block Copolymer Nanoassemblies for Controlled/Enhanced Drug Delivery. *Mol. Pharmaceutics* **2017**, *14*, 2460−2474.
(6) Delplace, V.; Nicolas, J. Degradable Vinyl Polymers for Biomedical Applications. *Nat. Chem.* **2015**, *7*, 771−784.
(7) Keller, S.; Toebes, B. J.; Wilson, D. A. Active, Autonomous, and Adaptive Polymeric Particles for Biomedical Applications. *Biomacromolecules* **2019**, *20*, 1135−1145.
(8) Zhou, K.; Wang, Y.; Huang, X.; Luby-Phelps, K.; Sumer, B. D.; Gao, J. Tunable, Ultrasensitive pH-Responsive Nanoparticles Targeting Specific Endocytic Organelles in Living Cells. *Angew. Chem., Int. Ed.* **2011**, *50*, 6109−6114.
(9) Liu, L.; Rui, L.; Gao, Y.; Zhang, W. Self-Assembly and Disassembly of a Redox-Responsive Ferrocene-Containing Amphiphilic Block Copolymer for Controlled Release. *Polym. Chem.* **2015**, *6*, 1817−1829.
(10) Hu, J.; Whittaker, M. R.; Li, Y.; Quinn, J. F.; Davis, T. P. The Use of Endogenous Gaseous Molecules (NO and CO2) to Regulate the Self-Assembly of a Dual-Responsive Triblock Copolymer. *Polym. Chem.* **2015**, *6*, 2407−2415.
(11) Bilalis, P.; Skoulas, D.; Karatzas, A.; Marakis, J.; Stamogiannos, A.; Tsimblouli, C.; Sereti, E.; Stratikos, E.; Dimas, K.; Vlassopoulos, D.; Iatrou, H. Self-Healing pH- and Enzyme Stimuli-Responsive Hydrogels for Targeted Delivery of Gemcitabine To Treat Pancreatic Cancer. *Biomacromolecules* **2018**, *19*, 3840−3852.
(12) Rikkou, M. D.; Patrickios, C. D. Polymers Prepared Using Cleavable Initiators: Synthesis, Characterization and Degradation. *Prog. Polym. Sci.* **2011**, *36*, 1079−1097.
(13) Percec, V.; Guliashvili, T.; Ladislaw, J. S.; Wistrand, A.; Stjerndahl, A.; Sienkowska, M. J.; Monteiro, M. J.; Sahoo, S. Ultrafast Synthesis of Ultrahigh Molar Mass Polymers by Metal-Catalyzed Living Radical Polymerization of Acrylates, Methacrylates, and Vinyl Chloride Mediated by SET at 25 °C. *J. Am. Chem. Soc.* **2006**, *128*, 14156−14165.
(14) Percec, V.; Popov, A. V.; Ramirez-Castillo, E.; Monteiro, M.; Barboiu, B.; Weichold, O.; Asandei, A. D.; Mitchell, C. M. Aqueous Room Temperature Metal-Catalyzed Radical Polymerization of Vinyl Chloride. *J. Am. Chem. Soc.* **2002**, *124*, 4940−4941.
(15) Rosen, B. M.; Percec, V. Single-Electron Transfer and Single-Electron Transfer Degenerative Chain Transfer Living Radical Polymerization. *Chem. Rev.* **2009**, *109*, 5069−5119.
(16) Zhang, N.; Samanta, S. R.; Rosen, B. M.; Percec, V. Single Electron Transfer in Radical Ion and Radical-Mediated Organic, Materials and Polymer Synthesis. *Chem. Rev.* **2014**, *114*, 5848−5958.
(17) Lligadas, G.; Grama, S.; Percec, V. Single-Electron Transfer Living Radical Polymerization Platform to Practice, Develop and Invent. *Biomacromolecules* **2017**, *18*, 2981−3008.
(18) Syrett, J. A.; Jones, M. W.; Haddleton, D. M. A Facile Route to End-Functionalised Polymers Synthesised by SET-LRP via a One-Pot Reduction/Thiol-ene Michael-Type Addition. *Chem. Commun.* **2010**, *46*, 7181−7183.
(19) Simula, A.; Nurumbetov, G.; Anastasaki, A.; Wilson, P.; Haddleton, D. M. Synthesis and Reactivity of α,ω-Homotelechelic Polymers by Cu(0)-mediated Living Radical Polymerization. *Eur. Polym. J.* **2015**, *62*, 294−303.
(20) Tsarevsky, N. V.; Matyjaszewski, K. Reversible Redox Cleavage/Coupling of Polystyrene with Disulfide or Thiol Groups Prepared by Atom Transfer Radical Polymerization. *Macromolecules* **2002**, *35*, 9009−9014.
(21) Tsarevsky, N. V.; Matyjaszeweski, K. Combining Atom Transfer Radical Polymerization and Disulfide/Thiol Redox Chemistry: A Route to Well-Defined (Bio)degradable Polymeric Materials. *Macromolecules* **2005**, *38*, 3087−3092.
(22) Siegwart, D. J.; Leiendecker, M.; Langer, R.; Anderson, D. G. Automated ARGET-ATRP Accelerates Catalyst Optimization for the Synthesis of Thiol-Functionalized Polymers. *Macromolecules* **2012**, *45*, 1254−1261.
(23) Yoshimoto, K.; Hirase, T.; Madsen, J.; Armes, S. P.; Nagasaki, Y. Non-Fouling Character of Poly[2-methacryloyloxy)ethyl Phosphorycholine]-Modified Gold Surfaces Fabricated by the 'Grafting to' Method: Comparison of its Protein Resistance with Poly(ethylene glycol)-Modified Gold Surfaces. *Macromol. Rapid Commun.* **2009**, *30*, 2136−2140.
(24) Warren, N. J.; Muise, C.; Stephens, A.; Armes, S. P.; Lewis, A. L. Near-Monodisperse Poly(2-(methacryloyloxy)ethyl Phosphorylcholine)-Based Macromonomers Prepared by Atom Transfer Radical Polymerization and Thiol-ene Click Chemistry Novel Reactive Steric Stabilizers for Aqueous Emulsion Polymerization. *Langmuir.* **2012**, *28*, 2928−2936.
(25) Li, S.; Ye, C.; Zhao, G.; Zhang, M.; Zhao, Y. Synthesis and Properties of Monocleavable Amphiphilic Comblike Copolymers with Alternating PEG and PCL Grafts. *J. Polym. Sci., Part A: Polym. Chem.* **2012**, *50*, 3135−3148.
(26) Su, X.; Ma, B.; Hu, J.; Yu, T.; Zhuang, W.; Yang, L.; Li, G.; Wang, Y. Dual-Responsive Doxorubicin-Conjugated Polymeric Micelles with Aggregation-Induced Emission Active Bioimaging and Charge Conversion for Cancer Therapy. *Bioconjugate Chem.* **2018**, *29*, 4050−4061.
(27) Kang, E. T.; Neoh, K. G.; Li, M.; Cai, T. Preparation of Stimuli Responsive Polycaprolactone Membranes of Controllable Porous Morphology via Combined Atom Transfer Radical Polymerization, Ring-Opening Polymerization and Thiol-yne Click Chemistry. *J. Mater. Chem.* **2012**, *22*, 16248−16258.
(28) Li, C.; Madsen, J.; Armes, S. P.; Lewis, A. L. A New Class of Biochemically Degradable, Stimulus-Responsive Triblock Copolymer Gelators. *Angew. Chem., Int. Ed.* **2006**, *45*, 3510−3513.
(29) Fritze, U. F.; Craig, S. L.; von delius, M. Disulfide-Centered Poly(methyl acrylates): Four Different Stimuli to Cleavage a Polymer. *J. Polym. Sci., Part A: Polym. Chem.* **2018**, *56*, 1404−1411.
(30) Rikkou-Kalourkoti, M.; Loizou, E.; Porcar, L.; Matyjaszewski, K.; Patrickios, C. S. End-Linked, Amphiphilic, Degradable Polymer Conetworks: Synthesis by Sequential Atom Transfer Radical Polymerization Using a Bifunctional, Cleavable Initiator. *Polym. Chem.* **2012**, *3*, 105−116.
(31) Rikkou-Kalourkoti, M.; Matyjaszewski, K.; Patrickios, C. S. Synthesis, Characterization and Thermolysis of Hyperbranched Homo- and Amphiphilic Co-polymers Prepared Using an Inimer Bearing a Thermolyzable Acylal Group. *Macromolecules* **2012**, *45*, 1313−1320.
(32) Syrett, J. A.; Mantovani, G.; Barton, W. R. S.; Price, D.; Haddleton, D. M. Self-Healing Polymers via Living Radical Polymerisation. *Polym. Chem.* **2010**, *1*, 102−106.
(33) Lee, M. E.; Gungor, E.; Armani, A. M. Photocleavage of Poly(methyl acrylate) with Centrally Located *o*-Nitrobenzyl Moiety: Influence of Environment on Kinetics. *Macromolecules* **2015**, *48*, 8746−8751.
(34) Johnson, J. A.; Baskin, J. M.; Bertozzi, C. R.; Koberstein, J. T.; Turro, N. J. Copper-Free Click Chemistry for the "In Situ" Crosslinking of Photodegradable Star Polymers. *Chem. Commun.* **2008**, *26*, 3064−3066.
(35) Johnson, J. A.; Finn, M. G.; Koberstein, J. T.; Turro, N. J. Synthesis of Photocleavage Linear Macromonomers by ATRP and Star Macromonomers by a Tandem ATRP-Click Reaction: Precursors to Photodegradable Model Networks. *Macromolecules* **2007**, *40*, 3589−3598.
(36) Elladiou, M.; Kalogirou, A. S.; Patrickios, C. S. Symmetrical Polymer Systems Prepared Using a Degradable Bifunctional Atom Transfer Radical Polymerization Initiator: Synthesis, Characterization and Cleavage. *J. Polym. Sci., Part A: Polym. Chem.* **2017**, *55*, 24342−2355.

DOI: 10.1021/acs.biomac.9b00892
Biomacromolecules 2019, 20, 3200−3210

(37) Johnson, J. A.; Lewis, D. R.; Díaz, D. D.; Finn, M. G.; Koberstein, J. T.; Turro, N. J. Synthesis of Degradable Model Networks via ATRP and Click Chemistry. *J. Am. Chem. Soc.* **2006**, *128*, 6564−6565.
(38) Zhang, Z. Y.; Zhang, Q. K.; Shen, Z.; Yu, J. P.; Wu, Y. W.; Fan, X. H. Synthesis and Characterization of New Liquid Crystalline Thermoplastic Elastomers Containing Mesogen-Jacketed Liquid Crystalline Polymers. *Macromolecules* **2016**, *49*, 475−482.
(39) Samanta, S.; Bogdanowicz, D. R.; Lu, H. H.; Koberstein, J. T. Polyacetals: Water-Soluble, pH-Degradable Polymers with Extraordinary Temperature Response. *Macromolecules* **2016**, *49*, 1858−1864.
(40) Enayati, M.; Jezorek, R. L.; Percec, V. A Multiple-stage Activation of the Catalytically Inhomogeneous Cu(0) Wire Used in SET-LRP. *Polym. Chem.* **2016**, *7*, 4549−4558.
(41) Rosen, B. M.; Lligadas, G.; Hahn, C.; Percec, V. Synthesis of Dendrimers Through Divergent Iterative Thio-Bromo "Click" Chemistry. *J. Polym. Sci., Part A: Polym. Chem.* **2009**, *47*, 3931−3939.
(42) Rosen, B. M.; Lligadas, G.; Hahn, C.; Percec, V. Synthesis of Dendritic Macromolecules Through Divergent Iterative Thio-Bromo "Click" Chemistry and SET-LRP. *J. Polym. Sci., Part A: Polym. Chem.* **2009**, *47*, 3940−3948.
(43) Nguyen, N. H.; Rosen, B. M.; Jiang, X.; Fleischmann, S.; Percec, V. New Efficient Reaction Media for SET-LRP Produced from Binary Mixtures of Organic Solvents and H_2O. *J. Polym. Sci., Part A: Polym. Chem.* **2009**, *47*, 5577−5590.
(44) Enayati, M.; Smail, R. B.; Grama, S.; Jezorek, R. L.; Monteiro, M. J.; Percec, V. The Synergistic Effect During Biphasic SET-LRP in Ethanol-Nonpolar Solvent-Water Mixtures. *Polym. Chem.* **2016**, *7*, 7230−7241.
(45) Enayati, M.; Jezorek, R. L.; Monteiro, M. J.; Percec, V. Ultrafast SET-LRP of Hydrophobic Acrylates in Multiphase Alcohol-Water Mixtures. *Polym. Chem.* **2016**, *7*, 3608−3621.
(46) Moreno, A.; Liu, T.; Ding, L.; Buzzacchera, I.; Galià, M.; Möller, M.; Wilson, C. J.; Lligadas, G.; Percec, V. SET-LRP in Biphasic Mixtures of Fluorinated Alcohols with Water. *Polym. Chem.* **2018**, *9*, 2313−2327.
(47) Moreno, A.; Galià, M.; Lligadas, G.; Percec, V. SET-LRP in Biphasic Mixtures of the Nondisproportionating Solvent Hexafluoroisopropanol with Water. *Biomacromolecules* **2018**, *19*, 4480−4491.
(48) Moreno, A.; Jezorek, R. L.; Liu, T.; Galià, M.; Lligadas, G.; Percec, V. Macromonomers, Telechelics and More Complex Architectures of PMA by a Combination of Biphasic SET-LRP and Biphasic Esterification. *Polym. Chem.* **2018**, *9*, 1885−1899.
(49) Moreno, A.; Liu, T.; Galià, M.; Lligadas, G.; Percec, V. Acrylate-macromonomers and Telechelics of PBA by Merging Biphasic SET-LRP of BA, Chain Extension with MA and Biphasic Esterification. *Polym Chem.* **2018**, *9*, 1961−1971.
(50) Grama, S.; Lejnieks, J.; Enayati, M.; Smail, R. B.; Ding, L.; Lligadas, G.; Monteiro, M. J.; Percec, V. Searching for Efficient SET-LRP Systems via Biphasic Mixtures of Water with Carbonates, Ethers and Dipolar Aprotic Solvents. *Polym. Chem.* **2017**, *8*, 5865−5874.
(51) Moreno, A.; Bensabeh, N.; Parve, J.; Ronda, J. C.; Cádiz, V.; Galià, M.; Vares, L.; Lligadas, G.; Percec, V. SET-LRP of Bio- and Petroleum-Sourced Methacrylates in Aqueous Alcoholic Mixtures. *Biomacromolecules* **2019**, *20*, 1816−1827.
(52) Moreno, A.; Lejnieks, J.; Galià, M.; Lligadas, G.; Percec, V. Acetone: a Solvent or a Reagent Depending on the Addition Order in SET-LRP. *Polym. Chem.* **2018**, *9*, 5411−5417.
(53) Jezorek, R. L.; Enayati, M.; Smail, R. B.; Lejnieks, J.; Grama, S.; Monteiro, M. J.; Percec, V. The Stirring Rate Provides a Dramatic Acceleration of the Ultrafast Interfacial SET-LRP in Biphasic Acetonitrile−Water Mixtures. *Polym. Chem.* **2017**, *8*, 3405−3412.
(54) Smail, R. B.; Jezorek, R. L.; Lejnieks, J.; Enayati, M.; Grama, S.; Monteiro, M. J.; Percec, V. Acetone−Water Biphasic Mixtures as Solvents for Ultrafast SET-LRP of Hydrophobic Acrylates. *Polym. Chem.* **2017**, *8*, 3102−3123.
(55) Moreno, A.; Grama, S.; Liu, T.; Galià, M.; Lligadas, G.; Percec, V. SET-LRP Mediated by TREN in Biphasic Water−Organic Solvent Mixtures Provides the Most Economical and Efficient Process. *Polym. Chem.* **2017**, *8*, 7559−7574.
(56) Liu, B.; Thayumanavan, S. Substituent Effects on the pH Sensitivity of Acetals and Ketals and Their Correlation with Encapsulation Stability in Polymeric Nanogels. *J. Am. Chem. Soc.* **2017**, *139*, 2306−2317.
(57) Whitfield, R.; Anastasaki, A.; Truong, N. P.; Wilson, P.; Kempe, K.; Burns, J. A.; Davis, T. P.; Haddleton, D. M. Well-Defined PDMAEA Stars via Cu(0)-Mediated Reversible Deactivation Radical Polymerization. *Macromolecules* **2016**, *49*, 8914−8924.
(58) Whitfield, R.; Anastasaki, A.; Nikolaou, V.; Jones, G. R.; Engelis, N. G.; Discekici, E. H.; Fleischmann, C.; Willenbacher, J.; Hawker, C. J.; Haddleton, D. M. Universal Conditions for the Controlled Polymerization of Acrylates, Methacrylates, and Styrene via Cu(0)-RDRP. *J. Am. Chem. Soc.* **2017**, *139*, 1003−1010.
(59) Jones, G. R.; Li, Z.; Anastasaki, A.; Lloyd, D. J.; Wilson, P.; Zhang, Q.; Haddleton, D. M. Rapid Synthesis of Well-Defined Polyacrylamide by Aqueous Cu(0)-Mediated Reversible-Deactivation Radical Polymerization. *Macromolecules* **2016**, *49*, 483−489.
(60) Moreno, A.; Garcia, D.; Galià, M.; Ronda, J. C.; Cádiz, V.; Lligadas, G.; Percec, V. SET-LRP in the Neoteric Ethyl Lactate Alcohol. *Biomacromolecules* **2017**, *18*, 3447−3456.
(61) Fukuda, T. Fundamental Kinetic Aspects of Living Radical Polymerization and the Use of Gel Permeation Chromatography to Shed Light on Them. *J. Polym. Sci., Part A: Polym. Chem.* **2004**, *42*, 4743−4756.
(62) Gyarmati, B.; Némethy, Á.; Szilágyi, A. Reversible Disulphide Formation in Polymer Networks: A Versatile Functional Group from Synthesis to Applications. *Eur. Polym. J.* **2013**, *49*, 1268−1286.
(63) Pasparakis, G.; Manouras, T.; Vamvakaki, M.; Argitis, P. Harnessing Photochemical Internalization with Dual Degradable Nanoparticles for Combinatorial Photo-Chemotherapy. *Nat. Commun.* **2014**, *5*, No. 3623.
(64) Lligadas, G.; Enayati, M.; Grama, S.; Sherman, S. E.; Percec, V. Ultrafast SET-LRP with Peptoid Cytostatic Drugs as Monofunctional and Bifunctional Initiators. *Biomacromolecules* **2017**, *18*, 2610−2622.

DOI: 10.1021/acs.biomac.9b00892
Biomacromolecules 2019, 20, 3200−3210